This poster participates in OSP
Outstanding Student Poster Contest
Vol. 16, EGU2014
EGU2014-445
Vienna, Austria : 27 April- 02 May 2014

Modeling D region Electron Density Enhancement Due to Solar Flares and Comparison with Algiers VLF Receiver Data

Yasmina BOUDERBA (1), Samir NAIT AMOR (1) and Mouloud TRIBECHE (2)
(1) Research Center on Astronomy, Astrophysics and Geophysics (CRAAG), Algiers, Algeria (**yasminabdb@hotmail.com**).
(2) University of Sciences and Technology Houari Boumediene (USTHB), Algiers, Algeria.

CRAAG

Abstract: Solar flares cause additional ionization in the D layer of the ionosphere (60-90 Km), which appears as amplitude and phase perturbations on the VLF signal. In this work, we present results of the properties of the VLF signals perturbations (amplitude, phase, h' and β) and their dependences with solar flares flux (For the period: 2007-2012). In this analysis two VLF transmitters paths are chosen, a short path: NSC (45.9 KHz, 941 Km) and long path NRK (37.5 KHz, 3495 km). In addition to the VLF data analysis, a numerical modeling of the D layer ionization due to solar flares was made at different heights (65-80 km). Qualitatively, the data analysis showed that the perturbed signal behavior is different from one path to another. In fact, some solar flares are associated with decreasing amplitude and increasing phase, increasing amplitude and decreasing phase, and finally decreasing or increasing in both amplitude and phase. This behavior is independent on the solar flares flux, but it is closely related to the modal structure of the VLF signal. Numerical results show that the increasing solar flares flux leads to the increasing of electron density and thus reducing the reflection height of VLF signal. Therefore, the recovery times of perturbed signal depend on the reflection height lifetime. The comparison between the calculated and measured densities as a function of solar flares flux at different heights gives similar profiles. **Key words**: Solar flares, Lower ionosphere, VLF signal Electron density.

1. Introduction :

The ionosphere is a part of the Earth's atmosphere which contains ionized gas (Plasma). Among different layers of the ionosphere, the diurnal **D layer** (60-90 km), ensures the propagation of Very Low Frequency radio waves (**VLF: 3- 50 KHz**) **[Mitra 1974]**. As this layer undergoes changes due to solar flares, two VLF transmitters T_x signals are chosen in this work (**NSC**, **NRK**) to study the solar flares flux effects on the propagating paths to Algiers receiver R_x:**NSC (45.9 KHz, 941 Km)** as a short path(**d <1000 Km**). **NRK (37.5 KHz, 3495 km)** as a long path (**d ≥ 1000 Km**). From measured perturbations amplitudes and phase, the electron density enhancement is calculated using the **LWPC** code on one part, and the **Wait formula** on another part. In addition to the experimental study, we developed a numerical simulation of the disturbed ionosphere under solar X-ray flux using the simple **GPI** ionosphere model **[Glukhov et al 1992]**. The numerical results are compared then to the experimental values.

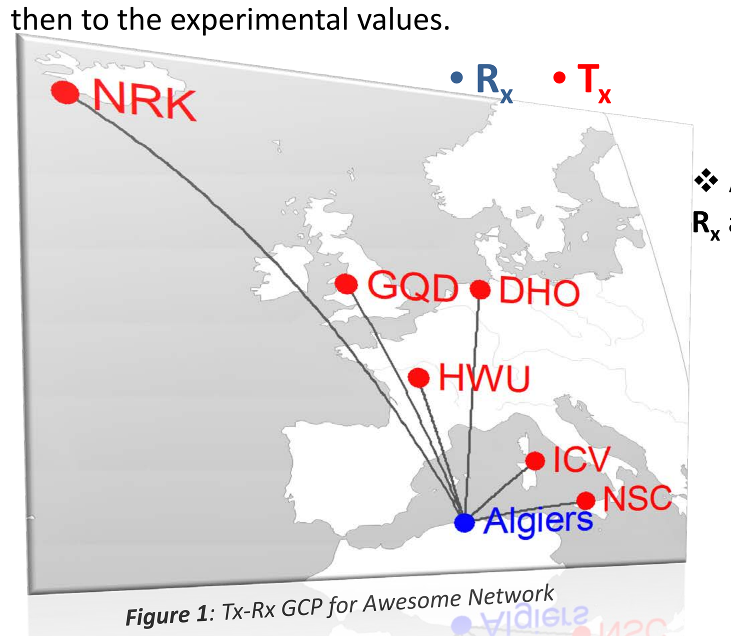

Figure 1: Tx-Rx GCP for Awesome Network

2. Experimental Setup

❖ An AWESOME R_x is installed at Algiers, Algeria (36.75 N, 03.47 E), along with the locations of VLF T_x and their great circle paths(GCP) to the R_x as seen in *Figure 1*.

R_x consists of:

- two magnetic loop antennas (N/S and E/W).
- a preamplifier
- a line receiver
- a GPS antenna
- a computer with data acquisition card.

It records and stores narrow-band data (the amplitude and phase of specific VLF T_x frequencies) and broadband data (100-kHz sampling). Data is synchronized to GPS with inherent 100 ns accuracy **[Nait Amor et al 2013]**.

3. Propagation of the waveguide:

❖ VLF waves propagate by successive reflections in the waveguide formed by the ground and the **D layer** (*Figure 2*).

- Quiet Sun: X-rays are absorbed over ***H*=74 km** (H: Reference reflection height of VLF waves).
- Active Sun(solar flare): X-rays penetrate down into the atmosphere ➡ N_e increased ➡ *H* is then reduced

Classification of solar flares (X-ray peak flux I_{max} (W/m²) :
10-6 ≤ C <10-5
10-5 ≤ M <10-4
10-4 ≤ X <10-3
as measured by **GOES** satellites **(0.1- 0.8 nm)**

Each X-ray class category is divided into a logarithmic scale from **1** to **9**.

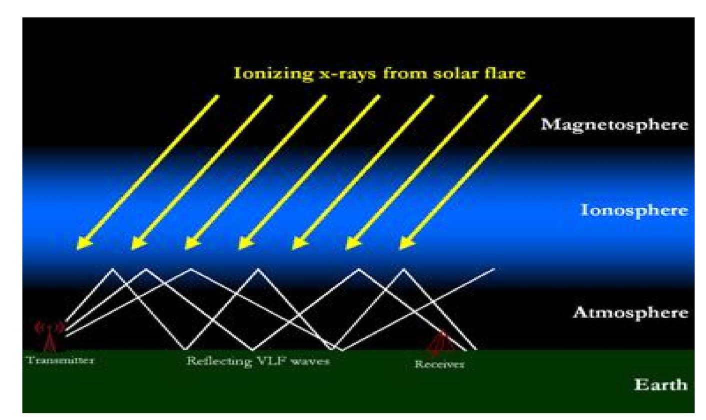

Figure 2: VLF Propagation in the waveguide (Earth-Ionosphere)

4. Processing and results

4. 1. Analysis of observational data

❖ The most prominent source of day time ionospheres perturbations is the X-ray solar flares. However they cause significant perturbations in both the received **amplitude** (*A*)and **phase *(φ)*** **Figure 3.**

❖Data analysis are done for solar flares flux recorded by **GOES** for the period: **2007- 2012.**

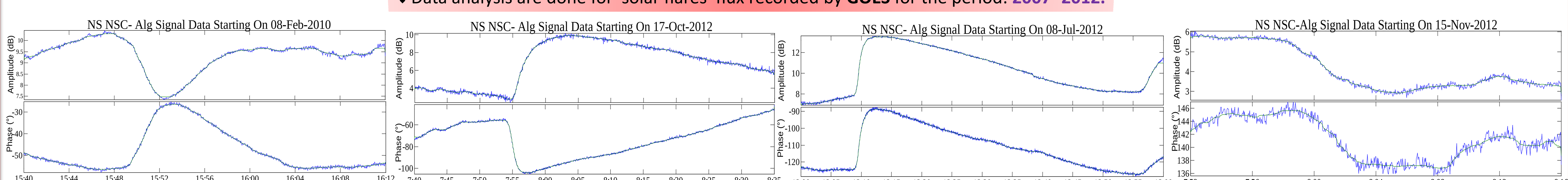

***Figure 3**: Some representative forms of VLF amplitude and phase signals recorded for distinct flares.*

The data analysis showed On **Figure 3**, that the perturbed signal has different forms **[Grubor et al 2008]**:

➢ a decreasing ***A*** and an increasing ***φ***

➢ an increasing ***A*** and a decreasing ***φ***

➢ a decreasing (or increasing) in both ***A*** and ***φ***

To understand the signal behavior in response to the solar flares, we use the Long Wave Propagation capability (**LWPC**) code **[Ferguson 1998]** to determine the perturbations in amplitude and phase. **The *Figure 4*,** gives the signal parameters (***A, φ***) plotted as function of the distance.

➢ Different forms of perturbed signal are recorded depending on the R_x location in addition to a zero perturbation. This is mainly due to the signal mode composition at the R_x location **[Nait Amor et al 2010]**.

➢ At short distance from the T_x(**d <1000 Km**): Several null points are observed.

➢ At far away from the T_x (**d ≥ 1000 Km**):These null points are spaced and thus a probability to record a signal perturbation (**+** or **-**) is important.

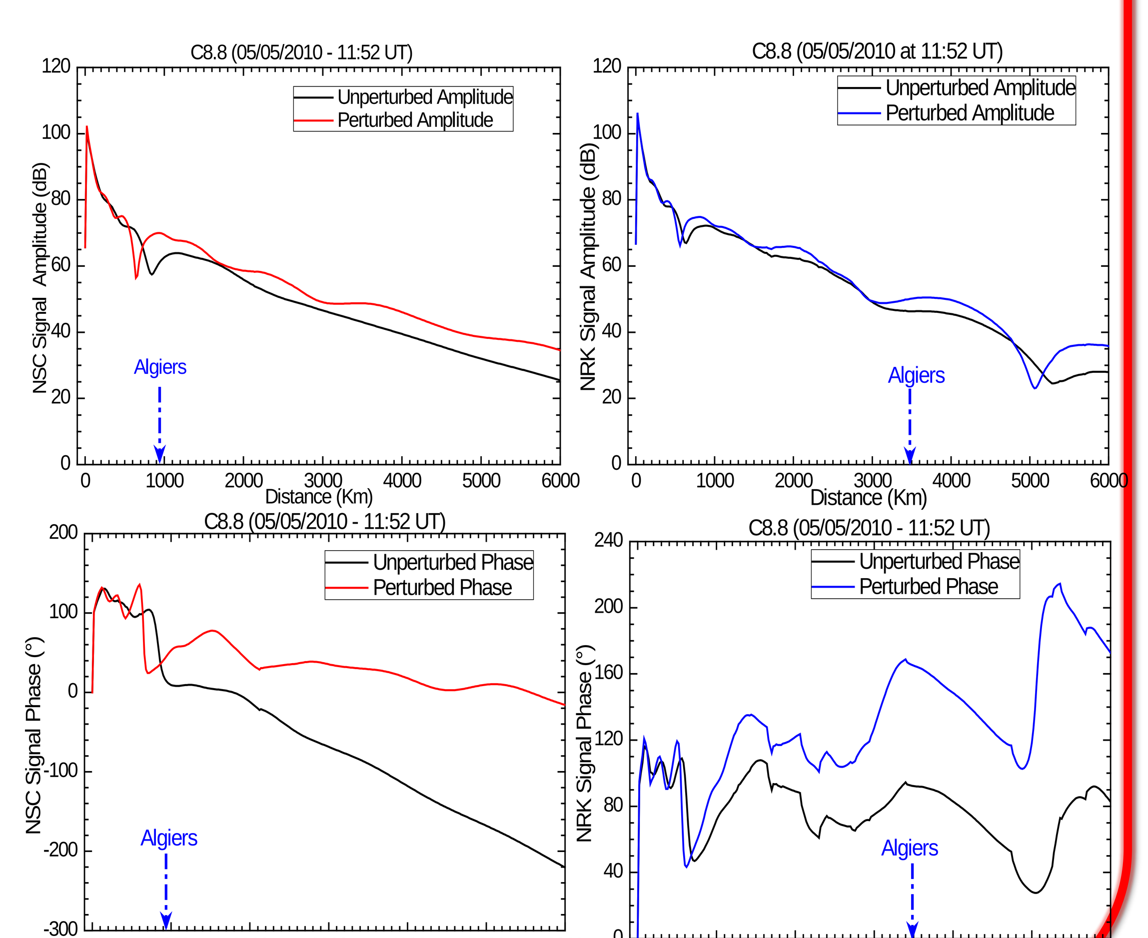

***Figure 4**: The behavior of unperturbed and perturbed **A** and **φ** as function of the distance from T_x for **NSC** and **NRK**.*

4. 2. Estimation of ΔA and Δϕ:

❖ The effect of solar flares on the signal parameters (***ΔA, Δφ***) is plotted as a function of the peak X-ray flux (I_{max}) in ***Figure 5*** for the two paths: **NSC** and **NRK**.

➢The perturbed VLF signal parameters (***ΔA, Δφ***) increase with the increasing of X-ray flux for the two GCP.

➢This increase results from the formation of a new reflecting height.

➢The variation of VLF signal parameters (***ΔA, Δφ***) is smoother for the long path: **NRK** than the short path: **NSC**.

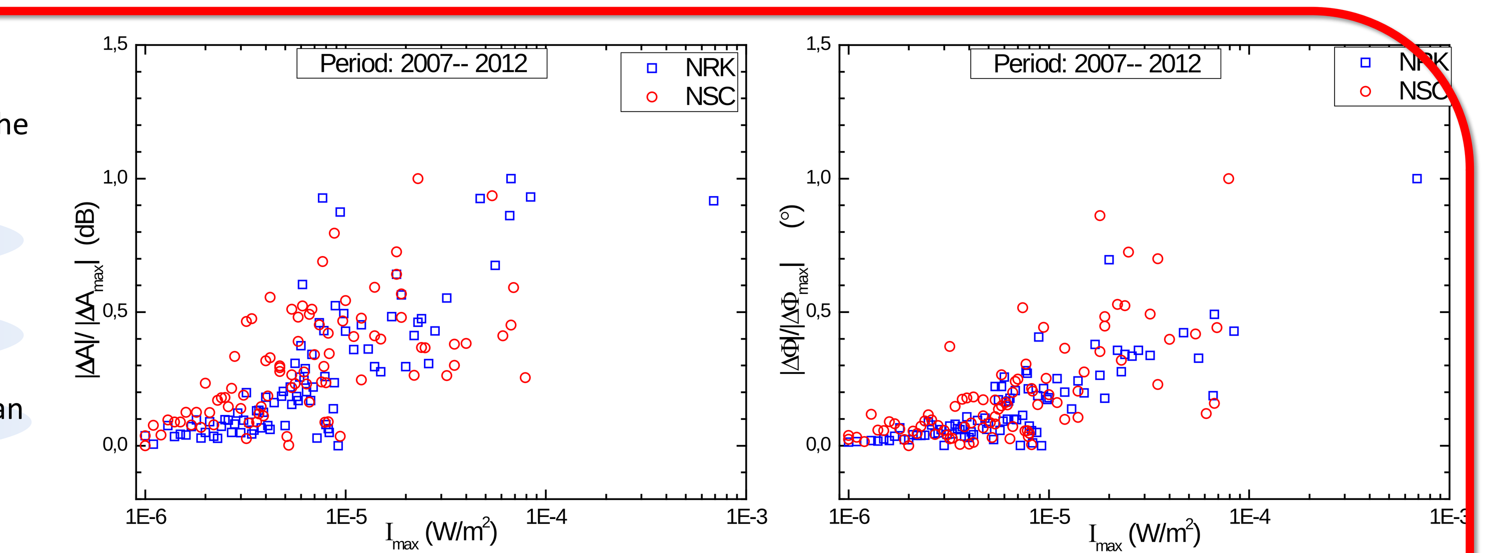

***Figure 5**: the perturbed VLF parameters (**ΔA ,Δφ**) as function of corresponding I_{max}*

4.3. Simulation technique using LWPC

❖ The **D layer** changes are characterized by two **Wait parameters** (***H', β***) which are obtained using the **LWPC** code.

H' (Km) :The effective reflection height
β (Km⁻¹) : The sharpness

➢ From *Figure 6*: ***H'*** is almost constant around **74 Km** (Ambient reference height) at low solar flare flux. The recombination overcomes the ionization process.

➢ ***H'*** decrease from low flux to about **64 Km** for high flux. This decrease is smoother in the **NRK** case than the **NSC** one.

➢ ***β*** increases from the ambient value (**0.3 Km⁻¹**) at lower flux to a saturation level about **0.49 Km⁻¹** for higher flux.

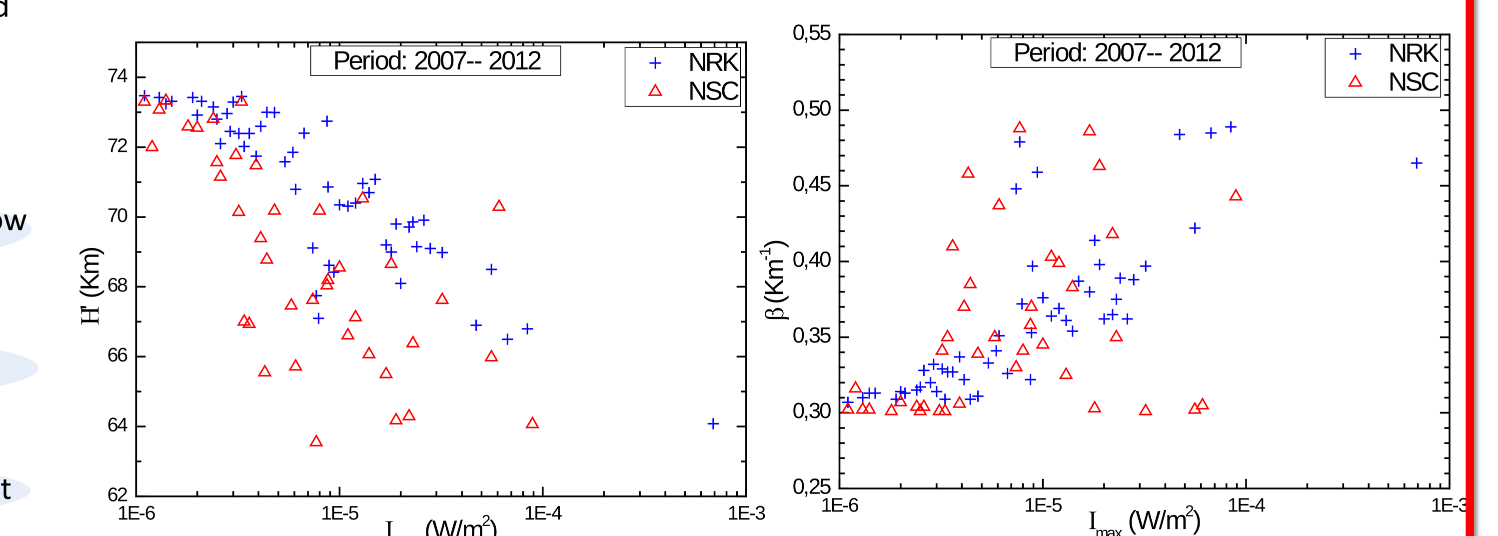

***Figure 6**: The variation of simulated (**H', β**) as a function of I_{max} for both GCP: **NSC** and **NRK**.*

❖ However, using Wait's formula **[1]** **[Wait and Spies 1964]**, we get the electron density N_e at **H = 70 Km** as shown in *Figure 7*. $Ne \propto e^{-\beta H'} e^{(\beta-0.15)H} \quad (cm^{-3})$ [1]

4.4. Numerical ionospheric model:

❖ The simplified Glokhov- Pasko- Ina (**GPI**) model is used to study the **D layer** modification due to solar flare flux. This is done by solving the differential equations **[2]** governing the equilibrium between D layer species densities by the **Finite Difference Method** :

$$\begin{cases} \dfrac{dN_e}{dt} = I + \gamma N^- - \beta N_e - \alpha_d N_e N^+ - \alpha_d^c N_e N_x^+ \\ \dfrac{dN^-}{dt} = \beta N_e - \gamma N^- - \alpha_i N^-(N^+ + N_x^+) \\ \dfrac{dN^+}{dt} = I + BN^+ - \alpha_d N_e N^+ - \alpha_i N^- N^+ \\ \dfrac{dN_x^+}{dt} = BN^+ - \alpha_d^c N_e N_x^+ - \alpha_i N^- N_x^+ \\ N_e + N^- = N^+ + N_x^+ \quad \text{(Quasi neutrality)} \end{cases} \qquad [2]$$

N_e, N^-, N^+, N_x^+ : are respectively electron, negative ions, positive ions and positive clusters density

γ, β, α_d, α_d^c, α_i, and ***B***: are the coefficients in terms of the neutral atom concentrations at different ***H*** (**NASA MSISE-90** atmospheric model).

I is the source of ionization (solar flares): $I \propto I_0 \left(1 - e^{t/t_1}\right) e^{t/t_2}$

I_0: is the X-ray solar flare flux as recorded by GOES (W/m²).
t_1 : is the onset time of the pulse function (s).
t_2 : is the recovery time of the pulse function (s).

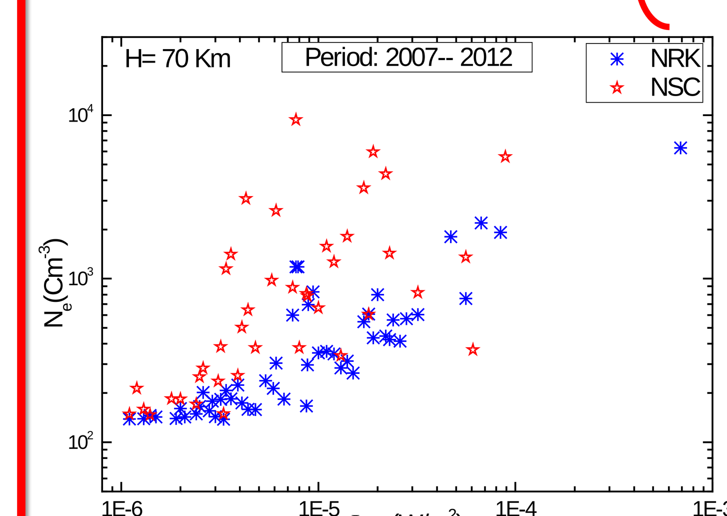

***Figure 7**: N_e (Wait model) **as a function** of I_{max} for both GCP: **NSC** and **NRK**.*

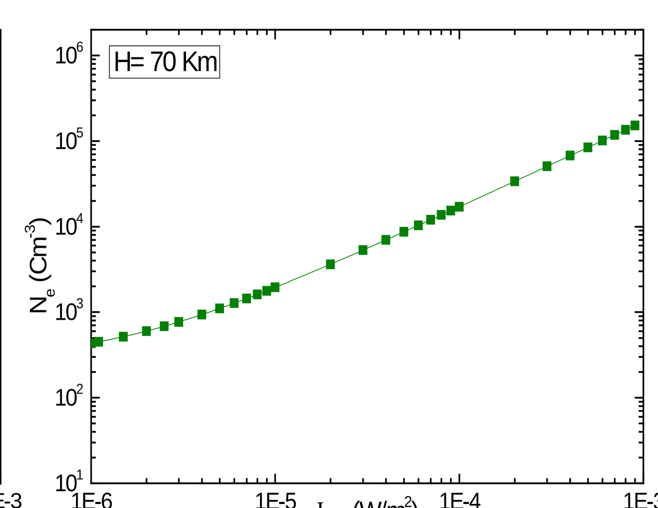

***Figure 8**: N_e (GPI model) dependence as function of I_{max}*

The Figure 7 , shows that at low solar flux N_e seems to be stable near the ambient density (Under unperturbed conditions), and then increases at higher solar flux.
It also appears that the increase is smoother for the long path **NRK** than the short path **NSC.**

The *Figure 8*, shows that the dependence of N_e obtained numerically using **GPI** model is similar to the experimental deduced N_e .

➢ Since at lower solar flare flux, the maximum absorption and ionization happen at higher altitude (above **74 Km**). The amount of ionization at lower altitude (bellow **74 Km**) is rapidly recombined.
➢ At higher solar flux, the ionization is important leading to reduce the reference height (bellow **74 Km**). Thus a significant signal perturbation is recorded.

5. Conclusion:

✓ The recording of signal perturbation due to solar flares appears to be independent on the solar X-ray flux. But it is closely related to the modal structure of the propagating signal.
✓ On the other hand, the perturbation parameters (***ΔA, Δφ***) increase with increasing solar flux.
✓ Data analyses show that long VLF path **NRK** is better than short VLF path **NSC** to study the solar flares effects on the D layer.
✓ And finally, the N_e dependence on the solar X-ray flux was found to be similar in both methods (numerical and experimental).

6. References:

- Ferguson, J. A.: Computer programs for assessment of long-wavelength radio communications, version 2.0. Technical document 3030, Space and Naval Warfare Systems Center, San Diego, 1998.
- Glukhov, V. S., Pasko, V. P., and Inan, U. S.: Relaxation of transient lower ionospheric disturbances caused by lightning-whistler-induced electron precipitation bursts, J. Geophys. Res., 97, 16971–16979, 1992.
- Grubor, D. P., Sulic, D. M., and Zigman, V.: Classification of X-ray solar flares regarding their effects on the lower ionosphere electron density profile, Ann. Geophys., 26, 1731–1740, 2008.
- Mitra, A. P.: Astrophysics and Space Science Library, vol. 46, D. Reidel Publishing Co., Dordrecht, 307 pp., 1974.
- NaitAmor, S., AlAbdoadaim, M. A., Cohen, M. B., Cotts, B. R. T., Soula, S., Chanrion, O., Neubert, T., and Abdelatif, T.: VLF observations of ionospheric disturbances in association with TLEs from the EuroSprite-2007 campaign, J. Geophys. Res., 115, A00E47, doi:10.1029/2009JA015026, 2010.
- NaitAmor, S., Cohen, M. B., Cotts, B. R. T., Ghalila, H., AlAbdoadaim, M. A., and Graf, K.: Characteristics of long recovery early VLF events observed by the North African AWESOME Network, J. Geophys. Res., 118, 1–8, 2013.
- Wait, J. R. and Spies, K. P.: Characteristics of the earth-ionosphere waveguide for VLF radio waves, NBS Tech. Note 300, 1964.